TIMEKEEPING AND TIME DISSEMINATION IN A DISTRIBUTED SPACE-BASED CLOCK ENSEMBLE

S. Francis
Zeta Associates Incorporated

B. Ramsey and S. Stein
Timing Solutions Corporation

J. Leitner, M. Moreau, and R. Burns
NASA Goddard Space Flight Center

R. A. Nelson
Satellite Engineering Research Corporation

T. R. Bartholomew
Northrop Grumman TASC

A. Gifford
National Institute of Standards and Technology

Abstract

This paper examines the timekeeping environments of several orbital and aircraft flight scenarios for application to the next generation architecture of positioning, navigation, timing, and communications. The model for timekeeping and time dissemination is illustrated by clocks onboard the International Space Station, a Molniya satellite, and a geostationary satellite. A mathematical simulator has been formulated to model aircraft flight test and satellite scenarios. In addition, a time transfer simulator integrated into the Formation Flying Testbed at the NASA Goddard Space Flight Center is being developed. Real-time hardware performance parameters, environmental factors, orbital perturbations, and the effects of special and general relativity are modeled in this simulator for the testing and evaluation of timekeeping and time dissemination algorithms.

1. INTRODUCTION

Timekeeping and time dissemination among laboratories is routinely achieved at a level of a few nanoseconds at the present time and may be achievable with a precision of a few picoseconds within the next decade. The techniques for the comparison of clocks in laboratory environments have been well established. However, the extension of these techniques to mobile platforms and clocks in space will require more complex considerations.

A central theme of this paper – and one that we think should receive the attention of the PTTI community – is the fact that normal, everyday platform dynamics can have a measurable effect on clocks that fly or ride on those platforms. It is generally appreciated that clocks moving on satellites with a high speed and at a high altitude are subject to relativistic effects. The principal example is the Global

Positioning System (GPS), where there is a net secular effect of 38 μs per day, a periodic effect with an amplitude of up to 46 ns, and a Sagnac effect of typically 100 ns for a stationary receiver on the geoid.

What is not so commonly known is that motion associated with, for example, aircraft can also result in measurable relativistic effects. We have measured such effects on recent flight tests and have modeled them via simulation. It is a surprise to many people that airborne platforms move fast enough, fly high enough, or cover enough distance to cause large enough effects to care about. In fact, atomic clocks can potentially exhibit relativistic effects even by their transport in a moving ground vehicle. For example, at a velocity of 65 km/h over a distance of 100 km, the time dilation correction is 10 ps.

This fact is one of the motivating factors for developing Two-Way Time Transfer (TWTT) technology adapted to moving platforms. Hence, it underlies much of our research program. This paper will cover background on clocks, timescales, and time dissemination, and will discuss some of the theoretical and experimental studies that we are doing in this area. In addition, we will provide a representative set of interesting simulation results specific to ground/space time-transfer.

2. TIME MEASUREMENT

The measurement and dissemination of time involves three distinct aspects: (1) the creation of a network of clocks, (2) the formation of a timescale, and (3) the development of algorithms for time transfer within a conventional spacetime coordinate system.

2.1 CLOCKS

A clock consists of a device capable of counting the periods of a repeatable phenomenon, whose motion or change of state is observable and obeys a definite law. Cesium or rubidium clocks of the type carried onboard GPS satellites have a precision on the order of a few parts in 10^{14}, or about 10 ns over a few hours. Hydrogen maser clocks in the laboratory offer a precision of a few parts in 10^{15} or 10^{16}. Technologies under development, such as those involving cesium fountain clocks, will improve these precisions.

The definition of the second describes a perfect clock, which is one that runs at the hyperfine frequency of the ground state of the cesium-133 atom at rest at a thermodynamic temperature of 0°K. This definition implies an isolated atom with no perturbations, which would make the clock unobservable. On the other hand, a real-world cesium clock permits the observation of the near ground-state hyperfine transition in many cesium atoms. Precision clocks have two types of imperfections: variations in period due to noise and those due to environmental influences.

There are two types of noise associated with the observation process – variations in the number of atoms that make a hyperfine transition due to the quantum nature of the transition process, and counting or shot noise of the detector. Both noise sources cause the phase of the clock to execute a random walk. The time of the clock diverges, but the frequency of the clock does not change. This type of noise is called white frequency noise. The clock signal is delivered to users through a system of synthesizers and output amplifiers that dominate the noise outside the bandwidth of the clock's control loop. Thermal noise in this signal processing circuitry causes the phase to change without diverging. This type of noise is called white phase noise and dominates the high frequency part of the clock's spectrum. The clock's noise perturbations are unavoidable, since they originate in the laws of quantum mechanics and thermodynamics.

In addition, there are environmental perturbations. These perturbations come from many sources. For example, the electromagnetic fields used to interrogate or confine the atoms and atom-atom collisions due to confinement both shift the energy levels away from their ground-state values. The sizes of the shifts are dependent on the operating conditions of the clock, such as temperature and pressure. As a result, environmental changes result in frequency changes of the clock. In principle, environmental perturbations can be made arbitrarily small and, thus, can be avoided.

2.2 TIMESCALES

Historically, timescales have been based on the rotation of the Earth on its axis (Universal Time), the revolution of the Earth around the Sun (Ephemeris Time), and the quantum mechanics of the atom (Atomic Time).

Atomic Time has been maintained continuously in various laboratories since 1955. Coordination of the atomic timescales was entrusted to the Bureau International de l'Heure (BIH) in 1961 at the Paris Observatory (OP). The 14th General Conference on Weights and Measures (CGPM) in 1971 approved the establishment of International Atomic Time (TAI) as the coordinate timescale whose unit interval is the second of the International System of Units (SI) as realized on the rotating geoid. In 1988, responsibility for TAI was transferred from the BIH to the International Bureau of Weights and Measures (BIPM). Approximately 250 cesium-beam standards and hydrogen masers located at observatories and national metrology laboratories around the globe contribute to the formation of TAI.

Coordinated Universal Time (UTC) is an atomic timescale that agrees in rate with TAI, but differs by an integral number of seconds. Presently, UTC is behind TAI by 32 seconds. UTC is maintained within 0.9 s of Universal Time (UT1), the astronomical timescale based on the rotation of the Earth, through the occasional addition of a leap second step. The decision to insert a leap second is made by the International Earth Rotation Service (IERS). Initially, UTC was kept close to UT1 by both frequency offsets and fractional step adjustments in order to aid celestial navigation by matching the broadcast atomic time signal with the Earth's rotation. The present UTC system of integral leap second steps without frequency offsets was adopted in 1972 so that an approximation to the epoch of UT1 and the interval of the SI second would be provided in the same emission **[1]**.

2.3 RELATIVISTIC ALGORITHMS

In parallel to the development of clocks and timescales, there must be a corresponding theoretical development of methods of time dissemination within an adopted spacetime coordinate system. These methods involve considerations of hardware properties, propagation effects, and relativity physics.

For relativistic time transfer, the distinction between coordinate time and proper time must be recognized. Coordinate time is a global coordinate that has the same value throughout all of space for a given event. In contrast, proper time is the time indicated by a clock in its own frame of reference and depends on the velocity of the clock and the gravitational potential at the location of the clock.

Relativity has become an important practical engineering consideration for modern precise timekeeping systems. Thus, far from being simply a textbook problem or merely of theoretical scientific interest, the analysis of both special and general relativistic effects on time measurement is an essential practical consideration. Neglect of these effects in satellite navigation systems would result in position errors on the order of tens of meters. For measurements with a precision at the nanosecond level, there are three relativistic effects that must be considered **[2, 3]**.

First, there is the effect of time dilation. The velocity of a moving clock causes it to appear to run slow relative to a clock on the Earth. GPS satellites revolve around the Earth with an orbital period of 11.967 hours and a velocity of 3.874 km/s. Thus on account of its velocity, a GPS satellite clock appears to run slow by 7 μs per day.

Second, there is the effect of the gravitational redshift, a frequency shift caused by the difference in gravitational potential. (The term "redshift" is generic regardless of sign, but for a satellite clock the frequency shift is actually a blueshift.) The difference in gravitational potential between the altitude of the orbit and the surface of the Earth causes the satellite clock to appear to run fast. At an altitude of 20,184 km, the clock appears to run fast by 45 μs per day.

The net effect of time dilation and gravitational redshift is that the satellite clock appears to run fast by approximately 38 μs per day when compared to a similar clock at rest on the geoid, including the effects of the velocity of rotation and the gravitational potential at the Earth's surface. This is an enormous rate difference for a clock with a precision of a few nanoseconds. To compensate for this large secular effect, the clock is given a fractional rate offset prior to launch of -4.465×10^{-10} from its nominal frequency of exactly 10.23 MHz, so that on average it appears to run at the same rate as a clock on the ground. The actual frequency of the satellite clock prior to launch is thus 10.229 999 995 43 MHz.

Although the GPS orbits are nominally circular, there is always some residual eccentricity. The eccentricity causes the orbit to be slightly elliptical. Thus, the velocity and gravitational potential vary slightly over one revolution and, although the principal secular effect is compensated by a rate offset, there remains a small residual variation that is proportional to the eccentricity. For example, with an orbital eccentricity of 0.02, there is a relativistic sinusoidal variation in the apparent clock time having an amplitude of 46 ns at the orbital period. This correction must be calculated and taken into account in the user's receiver.

The third relativistic effect is the Sagnac effect. The Sagnac correction in an Earth-Centered Earth-Fixed (ECEF) frame of reference is equivalent to a light-time correction for the receiver motion in an Earth-Centered Inertial (ECI) frame. For a stationary terrestrial receiver on the geoid, the Sagnac correction can be as large as 133 ns (corresponding to a GPS signal propagation time of 86 ms and a velocity of 465 m/s at the equator in the ECI frame). This correction is also applied in the receiver.

The analysis of signals used in cross-link ranging, time transfer among satellites and ground stations, and interoperability across constellations involves three steps: (1) a relativistic transformation from the proper time reading of the clock at the transmitter to the coordinate time of transmission in the adopted coordinate system; (2) calculation of the coordinate time of signal propagation, including both relativistic and nonrelativistic effects; (3) a relativistic transformation from the coordinate time of reception to the proper time reading of the clock at the receiver. In addition, all proper times must be corrected for "hardware" effects, such as signal noise and clock environment.

For cross-link ranging, the secular corrections must be modeled, especially for satellite systems that operate at different orbital altitudes. In addition, the relativistic eccentricity correction must be applied by receivers onboard the satellites themselves. Like those applied by ground receivers, these corrections will typically be on the order of tens of nanoseconds.

Analogous relativistic corrections will be needed in the European satellite navigation system, Galileo. Corrections beyond those already implemented in GPS will also be required if interoperability between the two systems is to be achieved, especially if signals from the two systems are combined in the receiver.

The GPS has served as a laboratory for doing physics at the 1-to-10 nanosecond level. The consistent application of relativity to GPS time and position measurements has been demonstrated by the operational precision of the system and by numerous experiments designed to test these individual effects over a wide range of conditions. GPS thus represents a model for the application of similar corrections across a broad spectrum of timekeeping systems. Relativistic effects on satellite clocks and signal propagation for a variety of orbits are compared in Table 1 **[2]**.

Table 1. Relativistic Effects on Satellite Clocks and Signal Propagation.

Constants									
Velocity of light	m/s	299792458							
Gravitational constant of Earth	km^3/s^2	398600.44							
Radius of Earth	km	6378.137							
J_2 oblateness coefficient		0.0010826							
Angular velocity of Earth rotation	rad/s	7.292E-05							
Geopotential on geoid U_0	m^2/s^2	6.264E+07							
U_0/c^2		-6.969E-10							
Satellite orbital properties									
Satellite		**ISS**	**TOPEX**	**Glonass**	**GPS**	**Galileo**	**Molniya**	**GEO**	**Tundra**
Semimajor axis	km	6766	7715	25510	26561.8	29994	26562	42164	42164
Eccentricity		0.01	0.001	0.02	0.02	0.02	0.722	0.01	0.2684
Inclination	deg	51.6	66.0	64.8	55.0	56.0	63.4	0.1	63.4
Argument of perigee	deg	0	0	0	0	0	250	0	270
Apogee altitude	km	456	1345	19642	20715	24216	39362	36208	47103
Perigee altitude	km	320	1329	18622	19652	23016	1006	35364	24469
Ascending node altitude	km	320	1329	18622	19652	23016	10507	35364	32748
Period of revolution	s	5539	6744	40549	43082	51697	43083	86164	86164
Mean motion	mrad/s	1.134	0.932	0.155	0.146	0.122	0.146	0.0729	0.0729
	rev/d	15.6	12.8	2.1	2.0	1.7	2.0	1.0	1.0
Mean velocity	km/s	7.675	7.188	3.953	3.874	3.645	3.874	3.075	3.075
Clock effects									
Secular time dilation	µs/d	-28.2	-24.7	-7.4	-7.1	-6.3	-7.1	-4.4	-4.4
Secular redshift	µs/d	3.5	10.4	45.1	45.7	47.3	45.7	51.0	51.0
Net secular effect	µs/d	-24.7	-14.3	37.7	38.6	41.1	38.6	46.6	46.6
Amplitude of periodic effect due to eccentricity	ns	12	1	45	46	49	1653	29	774
Peak-to-peak periodic effect due to eccentricity	ns	23	2	90	92	97	3306	58	1549
Secular oblateness contribution to redshift	ns/d	23.7	27.7	0.8	0.5	0.4	2.5	-0.1	0.2
Amplitude of periodic effect due to oblateness	ps	264	287	50	38	33	167	0	27
Peak-to-peak periodic effect due to oblateness	ps	528	573	99	76	65	334	0	54
Amplitude of periodic tidal effect of Moon	ps	0.0	0.0	1.0	1.2	1.8	1.2	6.1	6.1
Amplitude of periodic tidal effect of Sun	ps	0.0	0.0	0.5	0.5	0.8	0.5	2.7	2.7
Signal propagation									
Maximum Sagnac effect	ns	13	23	131	136	155	234	218	275
Gravitational propagation delay along radius	ps	0.8	2.5	-3.5	-4.7	-9.1	-4.7	-27.3	-27.3
Amplitude of periodic fractional Doppler shift	10^{-12}	13.1	1.1	7.0	6.7	5.9	241.1	2.1	56.5

3. TIME DISSEMINATION VIA GPS

The GPS program evolved from earlier systems and was formally chartered in 1973. The system was declared fully operational in 1995. The current GPS constellation consists of 28 Block II/IIA/IIR satellites. Each Block II/IIA satellite carries two cesium and two rubidium atomic clocks, while each Block IIR satellite carries three rubidium clocks. The fundamental clock frequency is 10.23 MHz. The satellite clocks and monitor station clocks contribute to the statistical formation of a continuous system time known as GPS Time, which is specified to be within 1 μs of UTC, except leap seconds are not inserted. After corrections for ionospheric and tropospheric propagation delays, relativity, and hardware effects are taken into account, GPS can provide an absolute time reference with a nominal precision of ≤ 25 ns. However, in practice the precision can be 10 ns or better.

The epoch of GPS Time is midnight of 5/6 January 1980. Therefore, GPS Time is behind TAI by a constant value of 19 s. Presently, GPS Time is also ahead of UTC by 13 s. This difference changes every time a leap second is inserted into UTC. GPS Time, TAI, and UTC are all realizations of the coordinate time in either the ECEF or ECI frame of reference (which by convention is the same in both frames).

GPS provides two types of global time service. The GPS satellites are considered to be a primary means of time transfer among clocks operating in widely separated National Metrology Institutions and other laboratories via common-view techniques with an uncertainty of a few nanoseconds **[4]**. In addition, GPS broadcasts a real-time prediction of UTC as maintained by the U.S. Naval Observatory (USNO).

The precision and universal availability of time as disseminated by GPS has produced a paradigm shift, with GPS evolving from a secondary source of time to a major time reference in itself. For example, GPS is the primary source of UTC for the Greenwich Time Signal service of the British Broadcasting Corporation (BBC) **[5]**.

4. SATELLITE CLOCK SIMULATIONS

To study the theoretical importance of various hardware-related biases, environmental factors, propagation delays, orbital perturbations, and relativistic effects on satellite clocks, a Two-Way Time Transfer Simulator has been developed as a MATLAB™-based tool that simulates a series of measured clock differences between moving platforms. Exchanges directly between two platforms or via a relay are supported. Noise contributions from a typical set of hardware components have been modeled, including special modules for clocks and modems. The platforms may have an arbitrary relative motion.

The simulation conducts a series of signal exchanges between the two platforms. Each platform transmits a timing signal according to a local clock's on-time marker (OTM). The simulator performs the calculations necessary to transform this local "hardware" proper time to an "ideal" proper time by correcting for the hardware biases. Then the coordinate time in an ECI reference frame is computed using a relativistic transformation. Based on this coordinate time of transmission, the simulator searches for a solution to the time of fight between the platforms. At the receiving platform, the calculations are inverted to compute the ideal proper time and the hardware proper time of reception. Finally, the platforms exchange their respective measurements of the difference between the local OTM and the received OTM, which are combined to determine the proper time difference between the clocks.

The key features of the simulation are its inclusion of relativistic effects, hardware noise, and arbitrary platform motion during the exchange. Relativistic effects are accounted for by the transformation between proper time and coordinate time in an ECI coordinate system. The simulator includes the time-

of-flight correction in the ECI reference frame, corresponding to the Sagnac effect in an ECEF reference frame.

Models for clock, modem, and measurement noise are implemented directly in the code. The simulator supports future modules to include variations in propagation delay. The clock noise is generated from a third-order model that includes noise densities for white phase noise, white frequency noise, frequency aging, and random-walk frequency aging. Noise densities for a high-performance cesium standard are used in the simulations presented in this paper. Additionally, the algorithm itself can accept clock steering inputs during the simulation. Modem noise is generated from a model that represents the performance of a commercially available satellite modem with special modifications to transmit low-latency OTM signals. Noise associated with the timer is based on the performance of a high-quality two-channel timer. Platform motion may be specified in several ways: directly via a set of waypoints that are time-stamped in hardware proper time, by a set of orbital elements, or generated algorithmically by a user-specified function.

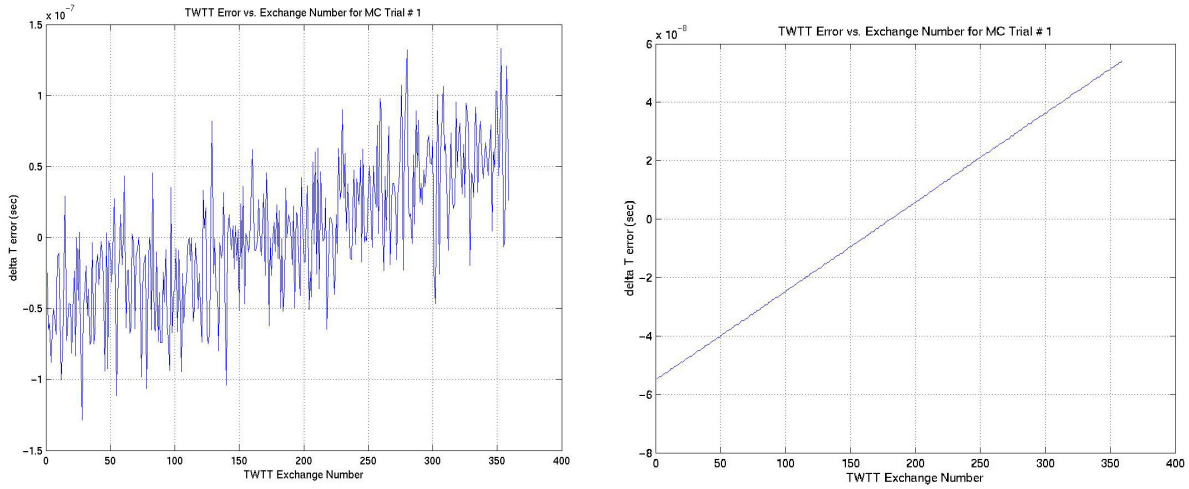

(a) *(b)*

Figures 1(a) and 1(b). Error between actual clock offsets and measured offsets for transfers between NIST and the ISS with (a) modem noise included and (b) modem noise not included.

Figures 1a and 1b show the simulation results for a fixed platform located at the National Institute for Standards and Technology (NIST) laboratories in Boulder, Colorado, USA and a moving platform in an orbit corresponding the International Space Station (ISS). Figure 1(a) includes the effects of modem noise, while Figure 1(b) shows the results when the modem noise is not included. The simulation time coincides with the portion of the orbit that is line-of-sight visible to NIST. Since the relative drift between the clocks themselves is removed from these plots, the resulting data show only the relativistic effects associated with the platform kinematics and gravitational potential and the noise introduced by the measurement and signal generation hardware. Analogous simulations were performed for an elliptical, highly inclined Molniya orbit and a geostationary orbit. Table 2 summarizes the range of errors for these simulations.

Table 2. Error Ranges for Three Orbits.

Orbit	Error Range
ISS	-55 to +53 ns
Molniya	-96 to +270 ns
Geostationary (GE-4 at 101° W)	+2.8 to +3.3 ns

5. FLIGHT TESTS

Geotemporal Sciences (GTS) group personnel have conducted two series of flight tests to investigate relativistic effects on clocks in subsonic airborne environments and to study and develop two-way time transfer technology for these flight regimes.

5.1 AT3 FLIGHT TESTS

Three flights were staged from Edwards AFB in the timeframe of March and April 2001 in support of the DARPA-funded Advanced Tactical Targeting Technology (AT3) program. The focus of this program was to develop and test a prototype system that will demonstrate that tactical (fighter and ground attack) aircraft can simultaneously accomplish their primary missions while satisfying SEAD/ESM requirements if each is equipped with an ESM sensor and processor interconnected by a single, real-time network **[6]**. A related requirement is that each participating aircraft must have sufficient knowledge of time and its own position to support the ultimate target geolocation accuracy requirement of 50 meters CEP.

The AT3 time recovery requirement was determined by Raytheon, the AT3 prime contractor, to be 8 ns peak relative time offset between participating aircraft. Because the time recovery mechanism was chosen to be passive via a GPS receiver (i.e., no GPS common view or active time transfer between platforms), the absolute time recovery requirement was 4 ns peak error relative to a selected timescale, such as UTC or GPS Time. The GTS group was asked to provide metrology support for these flights by using an atomic clock time reference onboard the T-39 test aircraft for comparison with the recovered GPS Time. Our approach was simply to fly a high-performance cesium clock and measure the GPS Time according to the GPS receiver relative to the atomic clock time throughout each flight using a time-interval analyzer.

The recorded time intervals were corrected for the relativistic effects on the clock due to the motion of the aircraft. The relativity corrections ΔT (flying clock – reference clock) for gravitational potential (redshift), velocity (time dilation), and Sagnac effect were accumulated over time increments Δt by the relations

$$\Delta T_g = \frac{g}{c^2}\sum_{i=1}^{N}(h_i - h_0)\,\Delta t_i \quad , \quad \Delta T_v = -\frac{1}{2c^2}\sum_{i=1}^{N} v_i^{\,2}\,\Delta t_i \quad , \quad \Delta T_s = -\frac{\omega}{c^2}\sum_{i=1}^{N} R_i^{\,2}\cos^2\phi_i\,\Delta\lambda_i \quad ,$$

respectively, where c is the speed of light, g is the acceleration of gravity, ω is the angular velocity of rotation of the Earth, $h - h_0$ is the relative height above the geoid, v is the velocity, R is the distance from the center of the Earth, ϕ is the latitude, and λ is the longitude over the path taken.

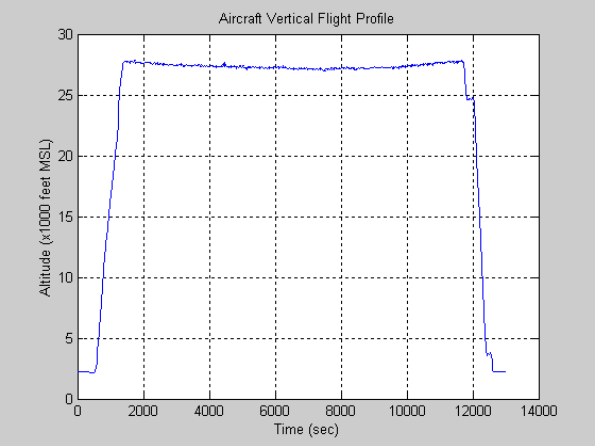

Figure 2. Vertical flight profile.

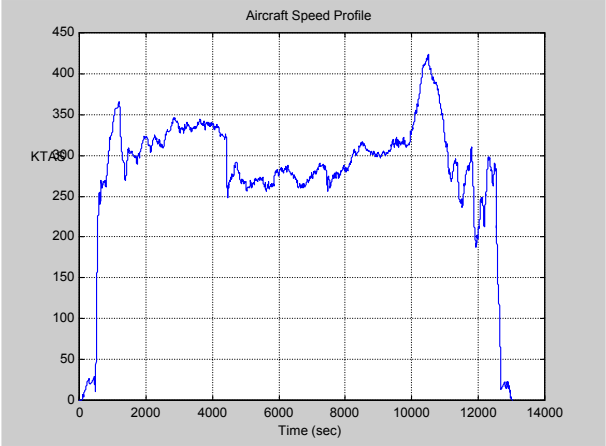

Figure 3. Speed profile.

The results of the first flight test are representative of many tactical military missions. The flight lasted 3.62 hours, during which the aircraft flew a "right triangle" profile at latitude 36° (of approximate dimensions 4° × 5° in the sequence east, north, and southwest) at an altitude of about 8,200 m (27,000 ft), as shown in Figure 2, and at a typical speed of about 560 km/h (300 knots), as shown in Figure 3.

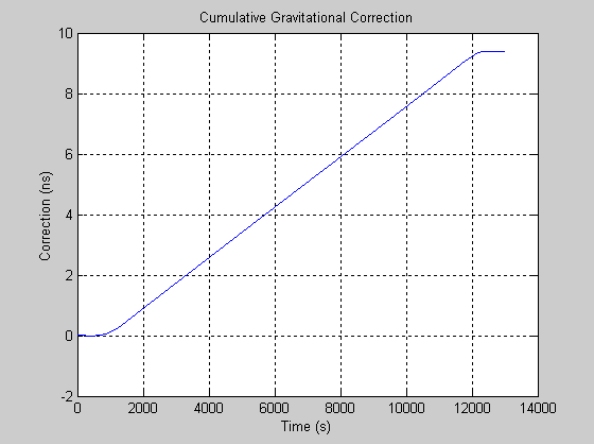

Figure 4. Gravitational potential correction (redshift).

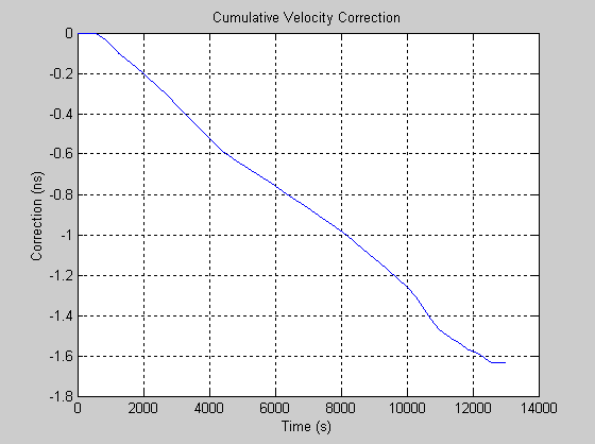

Figure 5. Velocity correction (time dilation).

From the recorded platform state vectors throughout the flight, the relativistic effects on the clock were determined analytically and were used to correct the time interval measurements between the GPS Time recovered from a GPS receiver (equivalent to coordinate time in the ECEF and ECI reference frames), and the cesium clock proper time. Figure 4 illustrates the effect due to the difference in gravitational potentials between the flight clock and ground clock. This effect, which caused the flight clock to run fast by 9.40 ns relative to the ground clock, was the dominant relativistic effect. Figure 5 illustrates the effect due to velocity, which caused the flight clock to run slow by 1.63 ns relative to the ground clock. Finally, Figure 6 illustrates the Sagnac effect, whose cumulative value of –0.10 ns is small because the flight covered a closed path bounding a small area. The total relativistic effect on the flight clock is illustrated

in Figure 7. As shown, when the flight was completed the flight clock was theoretically ahead of the clock on the ground by 7.67 ns. The actual flight clock data, when compared to the ground clock before and after the flight, was ahead by 7.3 ± 1.7 ns. The uncertainty represents the one-sigma variation in the pre-flight clock comparison data over a span of 6 hours, which is equivalent to the time the clocks were separated. The two additional flight tests during this series produced similar results. It is significant that the error in the clock closure would have been nearly five times the uncertainty in the measured clock data had relativity not been taken into account.

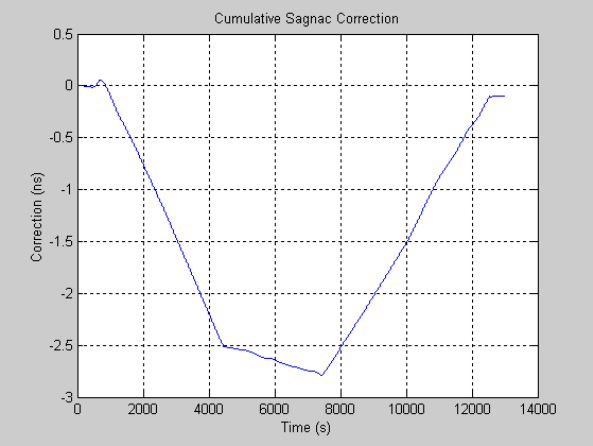

Figure 6. Sagnac correction.

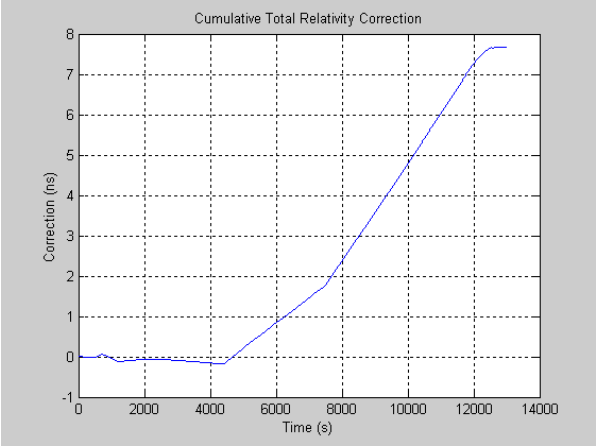

Figure 7. Total relativity correction.

5.2 C-135 Flight Tests

To further establish the modeling technique, we needed flights that produced greater relativity effects, i.e., flights that are faster, higher, or longer. Recent C-135 test flights staged from Wright-Patterson AFB during November 2002 helped to move the program in this direction.

A series of five flight tests were flown to evaluate two-way time transfer between a ground station and an airborne platform using both a direct line-of-sight radio-frequency (RF) link as well as a geostationary satellite communications relay. A companion paper **[7]** describes these flights in greater detail and provides Two-Way Satellite Time Transfer results. Our focus here is on the relativistic effects on the flight clock (again a high-performance cesium standard). Whereas during the AT3 flight tests we had no ability to measure flight clock behavior during the actual flight (GPS Time recovery was not sufficiently accurate for our purposes), the C-135 flight tests did give us an opportunity to monitor clock behavior throughout the entire flight by virtue of using the satellite time transfer method from the mobile platform.

The results of the first flight test, shown in Figure 8, are representative of our results in general. The aircraft flew for nearly 4 hours at an altitude of 11,000 m (35,000 ft) at an average speed of 790 km/h (425 knots). Our analytical results suggest that the flight clock should have run fast by 11.46 ns due to the difference in gravitational potential, slow by 3.03 ns due to velocity, and slow by 0.01 ns due to the net Sagnac effect, resulting in a total flight clock change of 8.42 ns (fast). Preliminary measured test results, after calibrating the estimated clock drift between the two clocks, showed that the flight clock ran fast by 8.3 ns relative to the ground clock. The difference between the predicted and measured values is consistent with clock noise on the order of a few parts in 10^{14} over the flight time interval. The anomalous dip of about 3 ns at time 9,000 s is not inconsistent with typical cesium clock behavior.

Similar artifacts of this magnitude were observed during comparisons between the same two clocks in the laboratory.

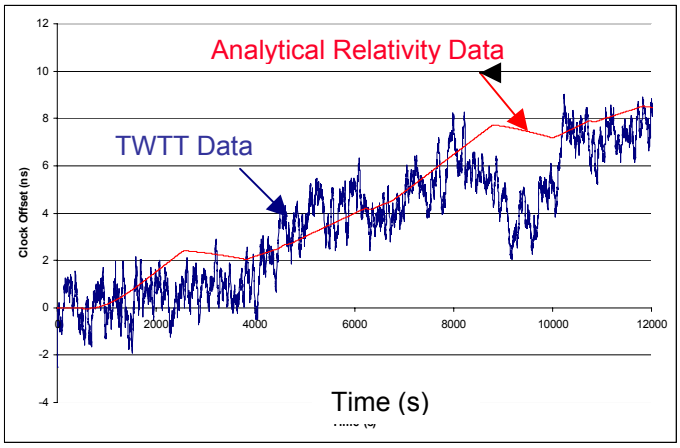

Figure 8. Comparison of total relativity correction and TWTT data.

6. FORMATION FLYING TESTBED (FFTB)

The satellite clock simulations and flight tests are iterative steps toward the realization of a distributed space-based clock ensemble. As the type and number of satellite formation flying mission concepts grows, so does the need for analysis and simulation of critical and enabling technologies associated with such missions. Precise time measurement, transfer, and synchronization are not only essential to achieve component stand-alone performance for navigation, control, and communications, but they provide the fundamental glue which enables the multiple spacecraft to act as a single coherent sensor. In contrast to traditional spacecraft missions, where measurements are computed from (perhaps) multiple sensors with delays that are well-known properties of the wire or fiber in the bus and controls are implemented similarly, the formation flying architecture is characterized by transfer of state vector data and control actuation commands that traverse through variable length RF or optical transmissions through open space. The variable and uncertain transmission times of the data causes errors in onboard relative navigation and larger errors in the formation control.

These issues give rise to the need to develop a high-fidelity hardware-in-the-loop simulation testbed environment, not only to assess the expected errors induced by geometric and environmental issues in particular mission scenarios, but additionally to develop procedures and algorithms to maintain performance robustly in the presence of such disturbances. The Formation Flying Testbed (FFTB) at NASA GSFC **[8]** is being developed initially as an integrated, hardware-in-the-loop, environment to validate formation flying architectures and algorithms for Earth-orbiting missions with GPS-in-the-loop. As the number of future formation flying missions of strategic interest to NASA has grown, the FFTB has been expanding to cover missions from Low-Earth Orbit through Lagrange point orbits, with an expanded interest in the end-to-end GN&C and communications-in-the-loop issues.

A schematic diagram of the hardware configuration of the FFTB is shown in Figure 9. Shaded items are responsible for generating the spacecraft environment. Specifically, the Environment Computer generates the spacecraft states $\mathbf{x}_i$; the GPS Signal Generator provides the RF input, which represents the signal from the GPS constellation (12 channels); and the Channel Simulator modifies the crosslink RF signal

(e.g., an RF transmission from satellite-1 to satellite-2 to introduce the effects of attenuation, Doppler frequency shift, and time delay). Thus, range and range rate measurements can be simulated based on measured RF signal characteristics. It should be noted that the Channel Simulator is an FY03 development project; consequently, it is not yet implemented. Currently intersatellite communication is simulated through IP-based communication between spacecraft processors, which represents ideal communications with no delay. Representative spacecraft hardware is indicated. GPS receivers onboard each spacecraft provide the spacecraft processor with an estimated absolute state, GPS observables, and a one-pulse-per-second time reference to the flight processor. Each flight processor must receive the GPS receiver input and communicate with the other members of the formation. Depending on the navigation and control scheme, one or more of the processors are responsible for running relative navigation and formation control processes. Control vectors $\mathbf{u}_i$ for each spacecraft are then passed back to the Environment computer for integration into the equations of motion.

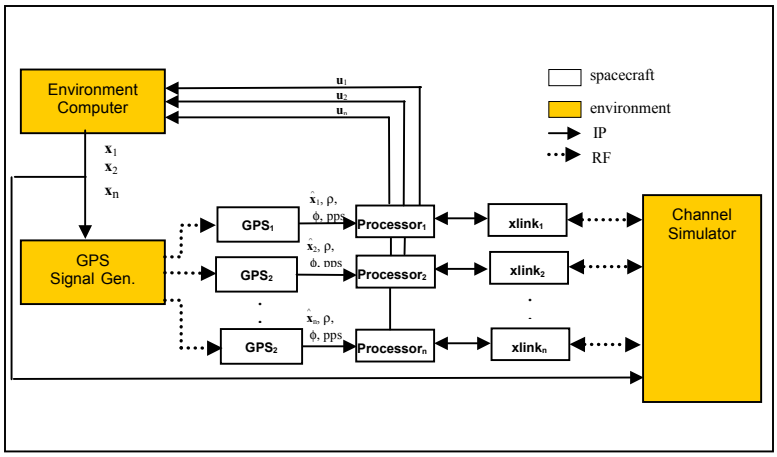

Figure 9. Formation Flying Testbed (FFTB) hardware design.

There are two major components of the TWTT process from the FFTB perspective: (1) the time transfer component, which is responsible for calculating the difference between the satellite clocks based on time-stamped intersatellite communications, and (2) the evaluation component, which has access to the true simulation time and evaluates how well the time transfer function is performing. Initially, for ease of integration, both components are hosted on the Environment computer; however, the time transfer component will eventually migrate to the spacecraft processors where it will interact directly with the crosslink hardware.

7. CONCLUSIONS

Timekeeping and time dissemination involves the development of clocks, timescales, and time transfer algorithms. This paper has called attention to the importance of relativistic corrections for time transfer. These corrections have been recognized as being essential to the successful operation of the GPS. Similar corrections will be needed for the consistent operation of other distributed space-based clock ensembles and for interoperability among satellite systems.

An experimental study of two-way time transfer to mobile platforms was performed by means of two series of aircraft flight tests in which relativistic corrections were measurable at the level of several

nanoseconds. It is noteworthy that closure between pre-flight and post-flight clock data would not have been obtained within the margin of experimental uncertainty if appropriate relativistic corrections were not included. Thus, it may be surprising to commonly held perceptions that aircraft dynamics can also result in measurable relativistic effects.

To study the theoretical importance of various hardware-related biases, environmental factors, propagation delays, orbital perturbations, and relativistic effects, a mathematical simulator has been formulated to model aircraft flight test and satellite scenarios. The model for timekeeping and time dissemination has been illustrated by clocks onboard the International Space Station, a Molniya satellite, and a geostationary satellite. In addition, a time transfer simulator integrated into the Formation Flying Testbed at the NASA Goddard Space Flight Center is being developed. Real-time hardware performance parameters, environmental factors, orbital perturbations, and the effects of special and general relativity are modeled in this simulator for the testing and evaluation of timekeeping and time dissemination algorithms.

REFERENCES

[1] R. A. Nelson, D. D. McCarthy, S. Malys, J. Levine, B. Guinot, H. F. Fliegel, R. L. Beard, and T. R. Bartholomew, 2001, *"The Leap Second: Its History and Possible Future,"* **Metrologia, 38**, 509-529.

[2] R. A. Nelson, 2002, **Handbook on Relativistic Time Transfer** (unpublished).

[3] N. Ashby and J. J. Spilker, Jr., 1996, *"Introduction to Relativistic Effects in the Global Positioning System,"* in **Global Positioning System: Theory and Applications,** edited by B. W. Parkinson and J. J. Spilker, Jr. (American Institute of Aeronautics and Astronautics, Washington, D.C.), Vol. 1, pp. 623-697.

[4] B. N. Taylor (editor), 2001, **The International System of Units (SI),** NIST Special Publication 330, 2001 edition (U.S. Government Printing Office, Washington, D.C.), 54 pp.

[5] J. A. McIlroy, 1993, *"The History of the Greenwich Time Signal from 1924 to the Present Day,"* **Engineering Science and Education Journal, 2**, 281-288.

[6] A. Gifford, S. Stein, S. Francis and R. A. Nelson, 2001, *"Relativity Prediction and GPS Time Recovery on an Airborne Platform,"* AT3 project report, August 2001.

[7] T. Celano, J. Warriner, S. Francis, A. Gifford, P. Howe, and R. Beckman, 2003, *"Two-Way Time Transfer to Airborne Platforms Using Commercial Satellite Modems,"* in these Proceedings, pp. 353-366.

[8] J. Leitner, 2001, *"A Hardware-in the-Loop Testbed for Spacecraft Formation Flying Applications,"* in Proceedings of IEEE Aerospace Conference, 10-17 March 2001, Big Sky, Montana, USA (IEEE Publication TH8542-TBR).

QUESTIONS AND ANSWERS

J. COMPARO (The Aerospace Corporation): Do you have any idea of what that discrepancy might have been between the two-way time transfer and your prediction?

SCOTT FRANCIS: We are still looking at that. The data are real new. There were some dynamics in the aircraft motion, obviously, that may or may not have been corrected for correctly in the two-way time transfer. It is an open question right now. So I don't know. The data are still very new and we are still processing a lot of it.